Spectrochimica Acta Part A: Molecular and Biomolecular Spectroscopy 97 (2012) 568–574

Contents lists available at SciVerse ScienceDirect

Spectrochimica Acta Part A: Molecular and Biomolecular Spectroscopy

journal homepage: www.elsevier.com/locate/saa

The synthesis, crystal structure and enhanced blue fluorescence emission of novel antipyrine derivatives

Yi-Feng Sun [a,b,*], He-Ping Wang [a], Yong Chen [a], Zhi-Yong Chen [a], Ji-Kun Li [b]

[a] Guangdong Provincial Public Laboratory of Analysis and Testing Technology, China National Analytical Center, Guangzhou 510070, PR China
[b] School of Chemistry and Chemical Engineering, Taishan University, Taian 271021, PR China

HIGHLIGHTS

- Novel antipyrine derivatives have been synthesized and characterized.
- X-Ray crystal structures of compound **1b** have been determined.
- Compound **1c** exhibits interesting fluorescence enhancement behavior.

GRAPHICAL ABSTRACT

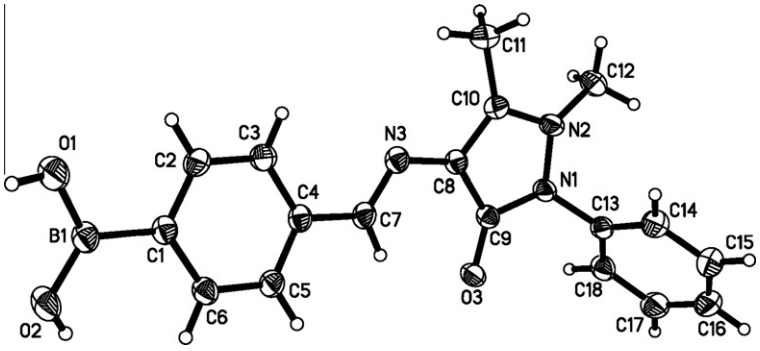

ARTICLE INFO

Article history:
Received 1 December 2011
Received in revised form 16 June 2012
Accepted 25 June 2012
Available online 10 July 2012

Keywords:
Antipyrine
2,2'-Bithiophene
Phenylboronic acid
Fluorescence enhancement
Synthesis
Crystal structure

ABSTRACT

Four new antipyrine derivatives were synthesized and characterized by elemental analysis, FT–IR, ^{1}H NMR, ^{13}C NMR spectroscopy, and a representative compound **1b** was confirmed based on the X-ray crystallographic analysis. The antipyrine–phenylboronic acid **1b** crystallizes in the monoclinic space group $P2_1/c$, and displays an *E* configuration about the C=N double bond. The absorption and fluorescence spectra of these compounds were investigated. Replacement of a six-membered phenyl group with a five-membered thienyl unit in the antipyrine derivatives resulted in a bathochromic shift approximately 21 nm, while the bithienyl system caused a strong bathochromic effect of 53 nm relative to the substituted phenyl groups. The bithienyl-antipyrine hybrid **1c** displayed a turn-on fluorescence response to water, acetic acid (HOAc) and sulfuric acid (H_2SO_4) in ethanol solution, but no fluorescence response toward alkali. Whereas the free compound was very weakly fluorescent in ethanol, the addition of water, HOAc and H_2SO_4 leads to an appearance of strong blue fluorescence and a dramatic increase of emission intensity.

Introduction

Antipyrine derivatives continue to generate great interest to medicine and science stemming from their wide range of pharmacological activities and clinical applications, including antifungal, antibacterial, antipyretic, analgesic, anti-inflammatory as well as antitumor activity [1,2]. At the same time, they have also been successfully used as a test for the effects of other drugs on the activity of drug-metabolising enzymes in the liver [3,4], as a chromogenic reagent for determination of bromate, urea [5], nitrate and phenol [6,7], and as chelating agents for coordinating, concentrating, and extracting of specific metal cations [8–13]. Much work has been focused mainly on the synthesis, structure characterization and biological evaluation of antipyrine derivatives [14–20], whereas only a few interesting fluorescence probes/chemosensors based

* Corresponding author at: School of Chemistry and Chemical Engineering, Taishan University, Taian 271021, PR China. Tel.: +86 20 37656300; fax: +86 20 87686511.
E-mail address: sunyf50@yahoo.com.cn (Y.-F. Sun).

1386-1425/$ - see front matter © 2012 Elsevier B.V. All rights reserved.
http://dx.doi.org/10.1016/j.saa.2012.06.047

on antipyrine and involving different mechanisms to induce spectral changes have been developed [21,22].

In our recent papers we reported on the synthesis and crystal structures of some antipyrine derivatives [23–25]. More recently, we found that a bithienyl-coumarin derivative displays three primary color emission bands, having maxima at 404, 524, and 697 nm, respectively, roughly corresponding to blue, greenish blue, and red light [26]. In view of the considerable importance of these compounds, we are thus interested in extending these studies to design and make materials with potential technological applications. Here, we wish to report the synthesis and spectroscopic characterization of new antipyrine derivatives. Specially, a bithienyl-antipyrine derivative (**1c**) has been synthesized, which is expected to possess some unique optical properties. Additionally, the molecular structure of **1b** was studied by the X-ray diffraction. The structures of target molecules are shown in Fig. 1.

Experimental

General

^{1}H NMR and ^{13}C NMR spectra were taken on a Bruker AVANCE-300 NMR spectrometer and chemical shifts expressed as δ (ppm) values with TMS as internal standard. Infrared spectra were measured over the region 400–4000 cm^{-1} with a Nicolet Magna 760 FT–IR instrument, with 4 cm^{-1} resolution. The samples were examined as KBr pellets. Element analysis was taken with a Perkin–Elmer 240 analyzer. Absorption spectra were determined on a Hitachi U-3900 UV–Vis scanning spectrophotometer. Fluorescence spectra measurements were performed on a Hitachi F-2500 spectrofluorimeter and the slit widths were 5 nm for both excitation and emission. Single crystal was characterized by Bruker Smart 1000 CCD X-ray single-crystal diffractometer. The melting points were determined with a WRS-1A melting point apparatus and are uncorrected. All reagents and chemicals are commercially available and used without further purification.

Synthesis of the antipyrine derivatives (*1*)

A mixture of 4-aminoantipyrine (2 mmol) and the appropriate aryl or heteroaryl aldehydes (2 mmol) anhydrous ethanol (30 mL) was heated under reflux for 3 h. After cooling, the solvent was removed under reduced pressure and the solid residues were recrystallized from ethanol to yield the pure products.

*1,5-Dimethyl-4-(3,5-di-tert-butyl-4-hydroxybenzylidene)amino-2-phenyl-1H- pyrazol-3(2H)-one (**1a**)*

Colorless crystals, yield 69%; mp 223–225 °C; ^{1}H NMR (300 MHz, $CDCl_3$/TMS) δ: 1.39 (s, 18H), 2.39 (s, 3H), 3.03 (s, 3H), 5.40 (s, 1H), 7.17–7.41 (m, 5H), 7.64 (d, J = 2.7 Hz, 2H), 9.61 (s, 1H). ^{13} C NMR (75 MHz, $CDCl_3$/TMS) δ: 10.25, 30.10, 30.24, 34.38, 36.16, 122.79, 124.02, 125.20, 126.56, 127.66, 129.09, 129.28, 135.04, 136.02, 151.52, 156.27, 158.59, 161.14. IR (KBr, cm^{-1}) v: 3537 (OH), 1647 (C=O), 1594 (C=N), 1109 (Ar–OH). Anal. calcd for $C_{26}H_{33}N_3O_2$: C 74.43, H 7.93, N 10.02; found: C 74.49, H 7.85, N 10.08.

*4-(1,5-Dimethyl-3-oxo-2-phenyl-2,3-dihydro-1H-pyrazol-4-yl)phenylboronic acid (**1b**)*

Pale yellow crystals, yield 63%; mp 248–250 °C; ^{1}H NMR (300 MHz, DMSO-d_6/TMS) δ: 2.47 (s, 3H), 3.19 (s, 3H), 7.36 (m, 3H), 7.55 (m, 2H), 7.77 (d, J = 8.1 Hz, 2H), 7.88 (d, J = 8.0 Hz, 2H), 8.15 (s, 2H), 9.65 (s, 1H). ^{13} C NMR (75 MHz, DMSO-d_6/TMS) δ: 9.74, 35.27, 116.31, 124.62, 126.14, 126.89, 129.11, 134.39, 134.52, 138.85, 152.20, 154.36, 159.54. IR (KBr, cm^{-1}) v: 3386 (OH), 1614 (C=O), 1590 (C=N), 1333 (B–O). Anal. calcd for $C_{18}H_{18}BN_3O_3$: C 64.50, H 5.41, N 12.54; found: C 67.42, H 5.56, N 12.47.

*1,5-Dimethyl-2-phenyl-4-(2-(5-(2-thienyl)thienyl) methylidene)amino-1H-pyrazo-3(2H)-one (**1c**)*

Yellow solid, yield 55%; mp 193–195 °C; ^{1}H NMR (300 MHz, $CDCl_3$/TMS) δ: 2.37 (s, 3H), 3.05 (s, 3H), 6.95 (m, 1H), 7.06 (d, J = 3.6 Hz, 1H), 7.18 (m, 3H), 7.28 (m, 3H), 7.40 (t, J = 8.0 Hz, 2H), 9.78 (s, 1H). ^{13} C NMR (75 MHz, $CDCl_3$/TMS) δ: 9.13, 34.79, 117.32, 123.15, 123.36, 123.40, 124.11, 125.94, 126.97, 128.18, 130.31, 133.70, 136.52, 139.16, 142.57, 149.34, 150.44, 159.79. IR (KBr, cm^{-1}) v: 1641 (C=O), 1579 (C=N). Anal. calcd for $C_{20}H_{17}N_3OS_2$: C 63.30, H 4.52, N 11.07; found: C 63.36, H 4.58, N 11.01.

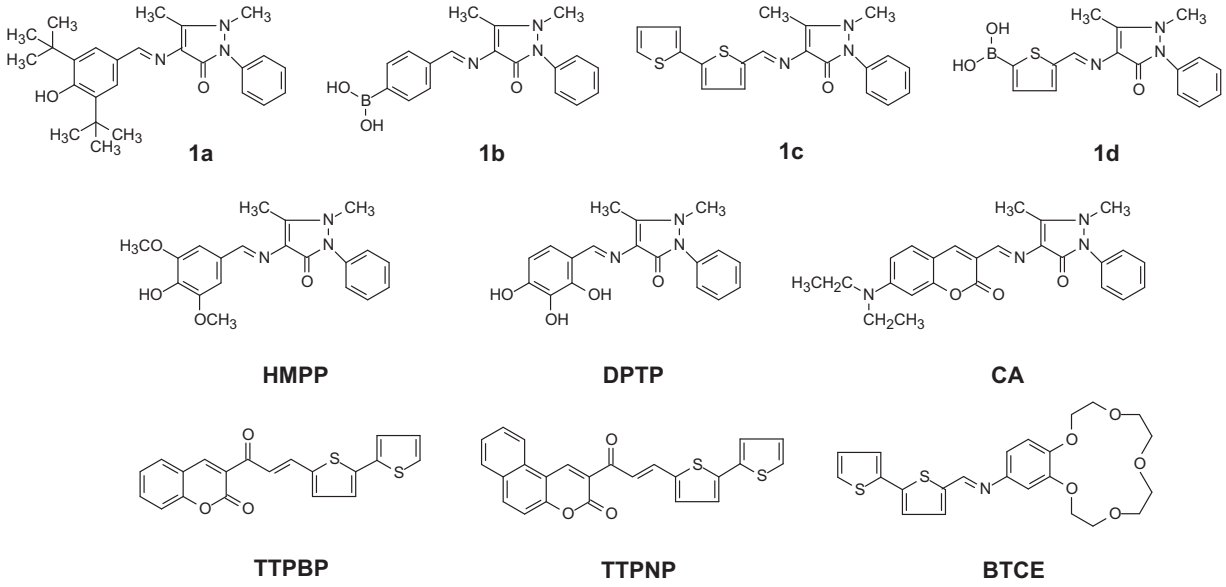

Fig. 1. The structures of the antipyrine and bithienyl derivatives.

*5-(1,5-Dimethyl-3-oxo-2-phenyl-2,3-dihydro-1H-pyrazol-4-yl)-2-thiophene boronic acid (**1d**)*

Green solid, yield 68%; mp > 250 °C; ^{1}H NMR (300 MHz, DMSO-d_6/TMS) δ: 2.41 (s, 3H), 3.17 (s, 3H), 7.38 (m, 3H), 7.47 (d, J = 3.9 Hz, 1H), 7.53 (t, J = 7.6 Hz, 2H), 7.65 (t, J = 3.6 Hz, 1H), 8.33 (s, 2H), 9.70 (s, 1H). ^{13} C NMR (75 MHz, DMSO-d_6/TMS) δ: 9.66, 35.26, 116.08, 124.65, 126.94, 129.13, 130.98, 134.46, 136.44, 148.26, 149.16, 151.63, 159.56. IR (KBr, cm^{-1}) v: 3349 (OH), 1622 (C=O), 1581 (C=N), 1321 (B–O). Anal. calcd for $C_{16}H_{16}BN_3O_3S$: C 56.32, H 4.73, N 12.32; found: C 56.38 H 4.81, N 12.26.

X-ray crystallography

X-ray quality crystals of **1b** were obtained by evaporation of ethanol solution. The diffraction data were collected on a Bruker Smart Apex 1000 CCD X-ray single crystal diffractometer with a graphite monochromated Mo Kα radiation (λ = 0.071073 nm) at 298(2) K. The structure was solved by direct methods with SHELXS-97 program and refinements on F^2 were performed with SHELXL-97 program by full-matrix least-squares techniques with anisotropic thermal parameters for the non-hydrogen atoms. All H atoms were initially located in a difference Fourier map. The methyl H atoms were then constrained to an ideal geometry, with C–H = 0.096 nm and U_{iso}(H) = 1.5U_{eq}(C). The hydroxyl H atom was treated as a riding atom, with O–H = 0.082 nm and U_{iso}(H) = 1.5U_{eq}(O). All other H atoms were placed in geometrically idealized positions and constrained to ride on their parent atoms with C–H distances 0.093 nm and U_{iso}(H) = 1.2U_{eq}(C). A summary of the crystallographic data and structure refinement details is compiled in Table 1.

Results and discussion

Synthesis and characterization

The antipyrine derivatives (Fig. 1) were easily prepared with 55–69% yield by refluxing equimolar amounts of the properly substituted aryl or heteroaryl aldehydes with 4-aminoantipyrine in anhydrous ethanol.

Table 1
Crystal data and structure refinement.

Compound	**1b**
Empirical formula	$C_{18}H_{18}BN_3O_3$
Formula weight	335.16
Temperature (K)	298(2)
Crystal system,	Monoclinic
Space group	$P2_1/c$
Unit cell dimensions	
a (nm)	1.3990(6)
b (nm)	0.6624(3)
c (nm)	1.8751(9)
α (°)	90
β (°)	102.444(7)
γ (°)	90
Volume (nm^3), Z	1.6967(14), 4
D_{calc} (Mg/m^3)	1.312
Absorption coefficient (mm^{-1})	0.090
F (000)	704
Crystal size (mm)	0.23 × 0.16 × 0.12
θ range for data collection(°)	2.40–25.05
Limiting indices	$-16 \leqslant h \leqslant 13$ $-7 \leqslant k \leqslant 7$ $-15 \leqslant l \leqslant 22$
Reflections collected/unique	8425/3001 [R_{int} = 0.0283]
Max. and min. transmission	0.9893 and 0.9796
Data/restraints/parameters	3001/0/229
Goodness-of-fit on F^2	1.039
Final R indices [I > 2sigma(I)]	R_1 = 0.0393; wR_2 = 0.0998
R indices (all data)	R_1 = 0.0489; wR_2 = 0.1067
Extinction coefficient	0.0110(14)
Largest diff. peak and hole (e.nm^{-3})	211 and −149
CCDC	845710

All compounds have been fully characterized spectroscopically. The IR spectra of these compounds show sharp and intense peaks in the range of 1579–1594 and 1610–1647 cm^{-1} which can be attributed to $v_{C=N}$ and $v_{C=O}$ stretching modes respectively. The broad IR signal centered at 3349–3537 cm^{-1} obtained for the three compounds **1a**, **1b** and **1d** can be ascribed to the OH functional groups.

The signals of protons displayed chemical shifts and multiplicities corresponding to their surroundings. The ^{1}H NMR spectra of all compounds showed a well distinguishable intensive singlet signal at δ = 9.61–9.78 ppm for the imino proton (CH=N). Additionally, the **1a** gave a characteristic singlet at $\delta \sim$ 5.40 ppm in $CDCl_3$, which was assigned to the OH proton. Obviously, in the ^{1}H NMR spectra the $B(OH)_2$ group signal was observed as a slightly broadened singlet at δ 8.15 ppm for **1b**, at δ 8.33 ppm for **1d**.

*Crystal structure of **1b***

Compound **1b** crystallizes in monoclinic space group $P2_1/c$ with four molecules in the unit cell. As can be seen from Fig. 2, the molecule **1b** adopts an E configuration about the central C=N double bond and exists in the imine form, as observed in the similar antipyrine Schiff base analogues, namely, 4-[(1E)-(4-Hydroxy-3,5-dimethoxy benzylidene)-amino]-1,5-dimethyl-2-phenyl-2,3-dihydro-1H-pyrazol-3-one (HMPP) [23] and 1,5-Dimethyl-2-phenyl-4-[(1E)-(2,3,4-trihydroxybenzylidene)amino]-1H-pyrazol-3(2H)-one (DPTP) [25] (Fig. 1).

The dihedral angle between the pyrazole ring and the substituted phenyl ring (C1–C6) is 16.9°, larger than the value of 7.5° found in HMPP, but smaller than the value of 25.3° in DPTP. The mean planes of the pyrazole and phenyl (C13–C18) rings make a dihedral angle of 117.2°. Therefore, the molecule **1b** is not planar. Obviously, the N3–C7 (0.1273(2) nm) and O3–C9 (0.12412(19) nm) bonds feature C=N and C=O double bonds.

On the other hand, the phenyl ring (C1–C6) and the boron coordination group, which adopts a trigonal planar configuration, are not coplanar with a dihedral angle of 11.3°. Moreover, B1, O1 and O2 deviate from the phenyl ring (C1–C6) mean plane by 0.00249, 0.02853 and 0.01378 nm, respectively. The B1–O1 (0.1344(2) nm) and B1–O2 (0.1361(2) nm) distances are somewhat shorter than the bonds in 2-[2-(2-Methoxy-ethoxy)-ethoxy]-phenylboronic acid (0.1358(2) and 0.1381(2) nm) [27]. Additionally, the bond angles at the trigonal planar boron atoms are somewhat distorted from ideal values in a manner which makes all of the hydrogen bonds more linear. The C1–B1–O1 angle (117.39(16)°) is significantly smaller than C1–B1–O2 (123.62(15)°). And, the O1–B1–O2 angle is 118.93(15)°. Similar geometry has been observed in related organoboron acids [27,28].

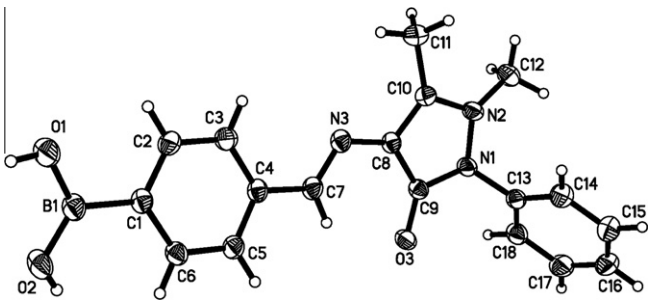

Fig. 2. The molecular structure of **1b**, showing the atom-labelling scheme. Displacement ellipsoids are drawn at the 50% probability level. H atoms are shown as small spheres of arbitrary radius.

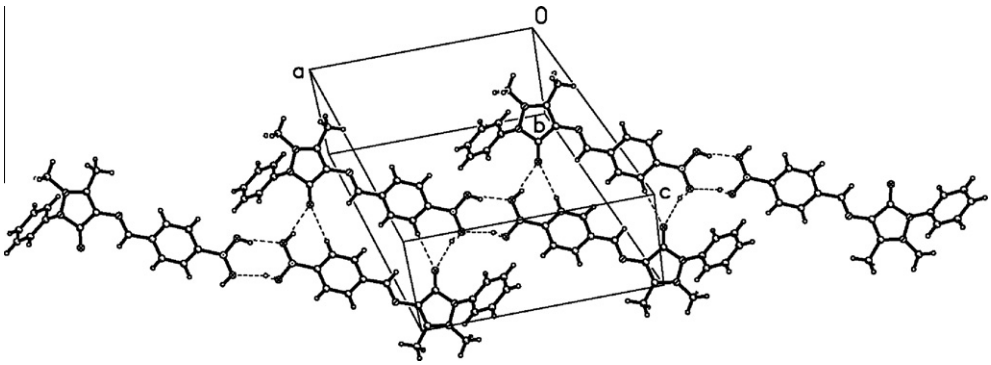

Fig. 3. The one-dimensional structure formed via hydrogen bonds in **1b**. The dashed lines indicate hydrogen bonds.

Generally, analogous to carboxylic acids, in boronic acids also, the hydroxyl groups may participate in hydrogen bonds. For example, the most common structural motif of phenylboronic acids is a cyclic dimer [29], which is formed by two units linked by intermolecular hydrogen bonds. As might be expected, such a basic subunit is also formed in the crystal structure of **1b**.

The molecules are linked by pair-wise self complementary O1–H1...O2 (O1–H1...O2^{i}: O–H = 0.0820 nm, H1...O2 = 0.2054 nm, O1...O2 = 0.2836 nm, O1–H1...O2 = 159°; symmetry code: (i) $-x-1, -y+2, -z+1$) hydrogen bonding interactions into a centrosymmetric dimer, with the formation of an eight-membered $R_2^2(8)$ ring motif as shown in Fig. 3. Further, the dimers are linked by intermolecular O–H...O and C–H...O hydrogen bonds (O2–H2...O3^{ii}: O–H = 0.0820 nm, H1...O2 = 0.2029 nm, O1...O2 = 0.2823 nm, O1–H1...O2 = 163°; C6–H6...O3^{ii}: C–H = 0.0930 nm, H6...O3 = 0.2555 nm, C6...O3 = 0.3319 nm, C6–H6...O3 = 140°; symmetry code: (ii) $-x, -y+2, -z+1$) into a one-dimensional structure extending along the *a*-axis (Fig. 3), which are further held together by the weak intermolecular C–H...N (C11–H11A...N3^{iii}: C–H = 0.0960 nm, H11A...N3 = 0.2610 nm, C11...N3 = 0.3565 nm, C11–H11A...N3 = 173°; symmetry code: (i) $-x, y+3/2, -z+1/2$) hydrogen bonds and π–π stacking interactions to form an extended network structure (Fig. 4).

Absorption and fluorescence spectra

The structures of the target molecules are shown in Fig. 1. All molecules (**1a–1d)** contain an antipyrine core. These molecules are related, but their chemical structures are differentiated by introducing various functional groups like substituted phenyl, thienyl and bithienyl into the antipyrine core. Such structural modification could be expected to result in some changes in the π-conjugated length and in the absorption and emission spectra.

These molecules are soluble in common organic solvents such as ethanol, dichloromethane and *N*,*N*-dimethylformamide. Among these molecules, the dilute ethanol solution of **1c** has the deepest color and appears yellow under natural light. UV–vis absorption spectra of these molecules in diluted ethanol solutions are given in Fig. 5, and the UV data are summarized in Table 2. Two to three absorption peaks could be observed in the absorption spectra of these four molecules in the wavelength range from 220 to

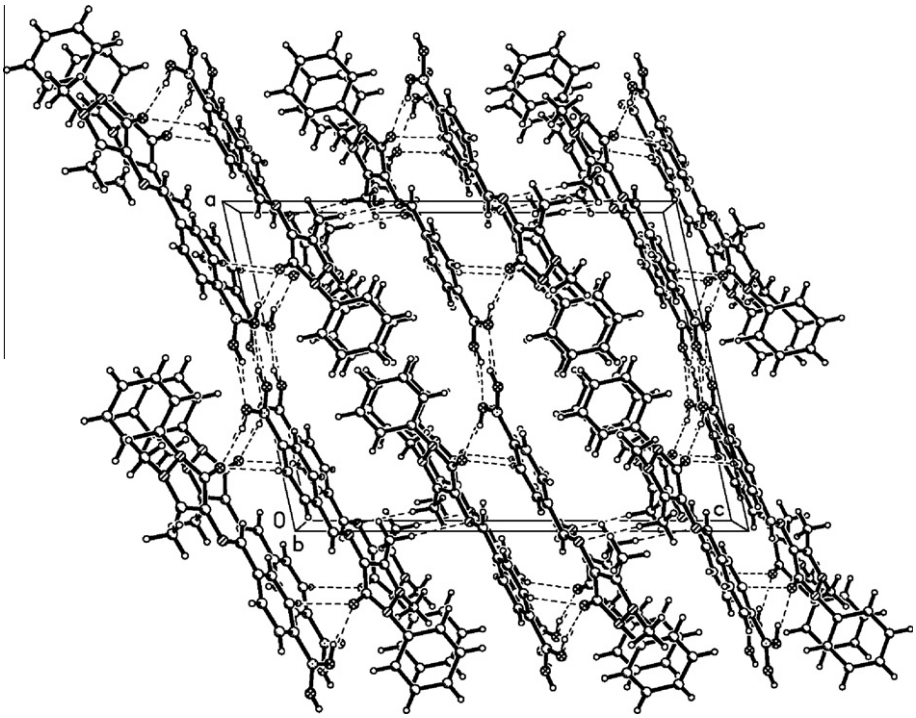

Fig. 4. A packing diagram for **1b**, viewed down the *b* axis. Dashed lines indicate hydrogen bonds.

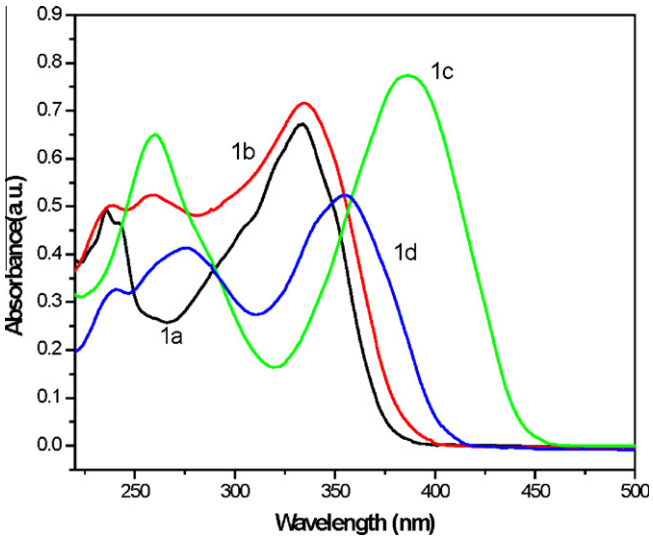

Fig. 5. Absorption spectra of compounds **1** in ethanol solution.

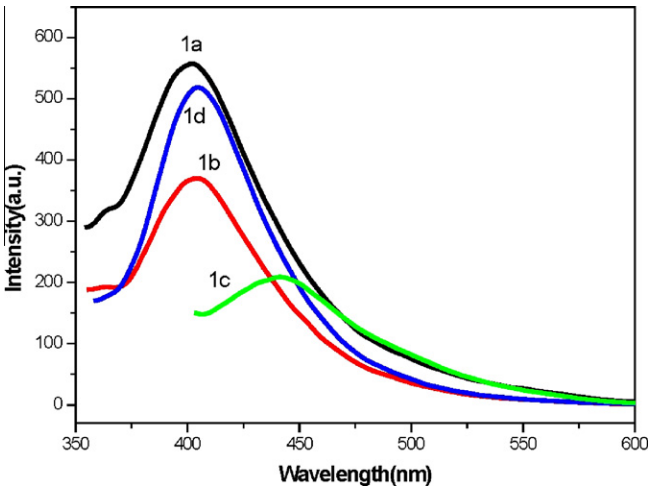

Fig. 6. Fluorescence spectra of compounds **1** in ethanol solution (excitation wavelength: 310 nm for **1a**, **1b** and **1d**, 350 nm for **1c**).

Table 2
Absorption and emission data for **1** in ethanol.

	Concentration/10^{-5} M	λ_a/nm	ε/M^{-1} cm^{-1}	λ_e/nm
1a	2.24	334	30000	402
		236	21900	
1b	2.46	334	29100	404
		260	21300	
		239	20400	
1c	2.16	387	35800	441
		260	30100	
1d	2.17	355	24100	405
		276	19100	
		241	15000	

500 nm. The first intense absorption band at longest wavelength is located at around 334–387 nm.

For the maximum absorption peaks of the first absorption band, there is a consequence: **1c** (387 nm) > **1d** (355 nm) > **1a**, **1b** (334 nm) (Fig. 5 and Table 2). As revealed in Fig. 5, clearly, both **1a** and **1b** have the same value of λ_{max}, while both **1b** and **1d** have the similar spectral shape, owing to their very similar structure. Furthermore, we noticed that when replacing 3,5-di-tert-butyl-4-hydroxyphenyl with a boronophenyl group, a change in the shorter wavelength part of the spectrum is observed. Concomitantly, the replacement of six-membered phenyl group with five-membered thienyl unit resulted in a red shift of approximately 21 nm in λ_{max}. Considering such a bathochromic shift, one can say that the electronic effect of thienyl group is stronger than that of the phenyl group. In fact, it is known that thiophene rings are π-excessive, and have a greater diene character than phenyl rings. Thus, thiophene rings are thought to facilitate changes in charge density upon excitation as a consequence of reduced aromaticity, which might explain the bathochromic shift.

It is worth noting that derivative **1c** featuring electron-rich bithienyl substituent, shows only two absorption bands at around 387 and 260 nm, and its value of λ_{max} with a high extinction coefficient (ε_{max} = 35800 M^{-1} cm^{-1}) is considerably more red-shifted than those of other antipyrine derivatives (Fig. 5 and Table 2). This is apparently related to the greater electron-donating ability of the end bithienyl unit. Therefore, it could be suggested that more π-electrons and more extended π-conjugated system may be involved in **1c** than those in others. The presence of an extended π-conjugated system in **1c** was also confirmed by the observation of a strong broad absorption in its UV–vis spectrum.

Additionally, as one would expect from the joining of the pyrazole ring to the conjugated bithienyl framework with a CH=N bridge, in comparison to that for bithiophene (λ_{max} = 303 nm) [30], λ_{max} for **1c** is red-shifted 84 to 387 nm. At the same time, the absorption bands of **1c** are red-shifted of 7–10 nm as compared to the bithienyl-containing Schiff base BTCE with two maximum centered at 380 and 250 nm [31]. In contrast, λ_{max} of **1c** is considerably blue-shifted with respect to those of coumarin-bithienyl hybrids (3-(3-(2-(thiophen-2-yl)thiophene-5-yl) prop-2-enoyl) -2*H*-1-benzopyrane-2-one (TTPBP) (λ_{max} = 436 nm) and 3-(3-(2-(thiophene-2-yl) thiophene-5-yl)prop-2-enoyl)-2*H*-1-naphtho[2,1-*b*]pyran-2-one (TTPNP) (λ_{max} = 445 nm)) [32] and coumarin–antipyrine hybrid (CA) (λ_{max} = 453 nm) [22], indicating the presence of a more extended π-conjugated system in three coumarin hybrids.

The fluorescence properties of compounds were investigated in ethanol solution at room temperature (excitation wavelength: 310 nm for **1a**, **1b** and **1d**, 350 nm for **1c**). The fluorescence spectra are shown in Fig. 6, and the fluorescence spectral data are summarized in Table 2. As expected, all antipyrine derivatives exhibit rather weak fluorescence due to the isomerization around the C=N bond, and have similar fluorescence spectra. The emission maxima for **1a**, **1b**, **1c** and **1d** appear at 402, 404, 441 and 405 nm, respectively. In comparison with **1a**, **1b** and **1d**, **1c** shows a ~36 nm red shift in λ_{max}. But, weak emission of **1c** is blue-shifted as compared to that observed for coumarin–antipyrine hybrid CA (500 nm) [22].

As will be shown, however, it is found that **1c** exhibits interesting fluorescence multi-responses to water, HOAc and H_2SO_4.

*Fluorescence enhancement behaviour of **1c***

The effect of solvents on the fluorescence of **1c** is investigated systematically by using aqueous binary solutions as the medium. In ethanol, **1c** showed interesting response sensitivities when water was added. In comparison to the data recorded in pure ethanol solution, the addition of water brought marked changes to the emission spectra of **1c**, although the absorption was slightly affected by the presence of water. Fluorescence emission wavelength and intensity of the solutions with different water fractions (vol%), as well as the fluorescence emission response photograph of **1c** in ethanol solution in the absence and presence of water are shown in

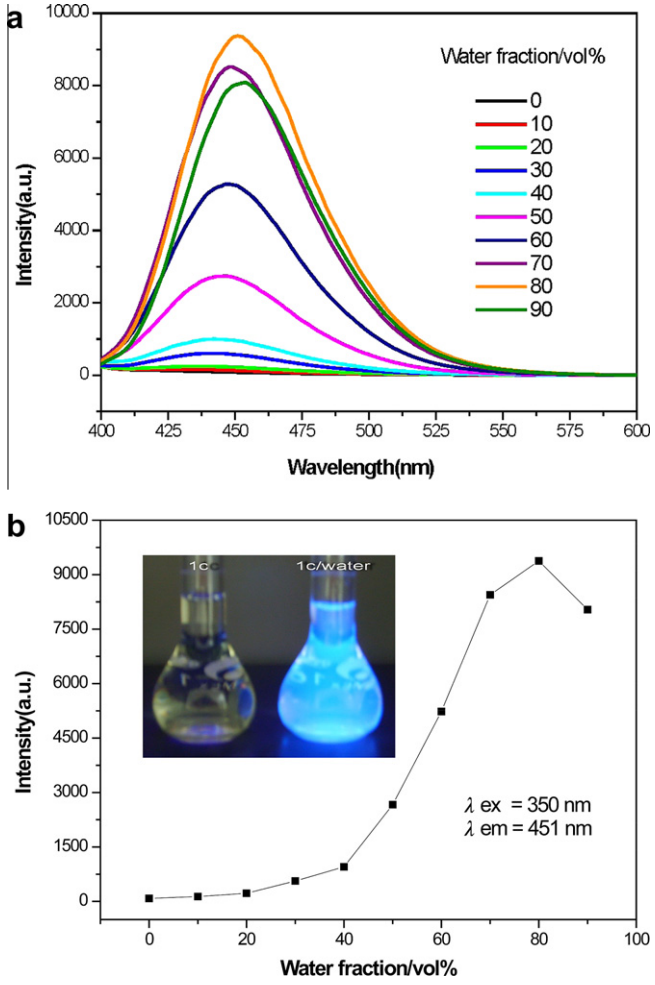

Fig. 7. (a) Fluorescence spectra of **1c** in ethanol–water mixtures (1.08×10^{-6} M). (b) Fluorescence intensity at 451 nm as a function of water fraction. *Inset*: photograph of **1c** in ethanol with and without addition of water under irradiation at 365 nm.

Fig. 7. As the water fraction increased, the change of fluorescence emission intensity exhibited a two-step process: first enhanced,

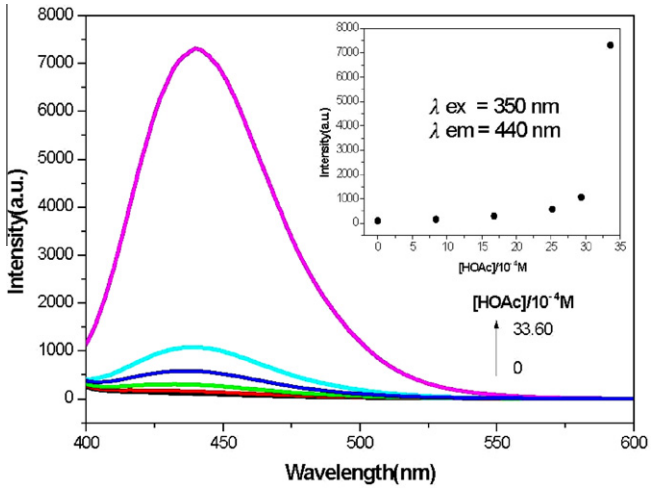

Fig. 8. Fluorescence spectra changes of **1c** in ethanol solution (1.08×10^{-6} M) upon addition of increasing concentrations of HOAc (0–33.60×10^{-4} M). *Inset*: fluorescence intensity at 440 nm as a function of HOAc concentration.

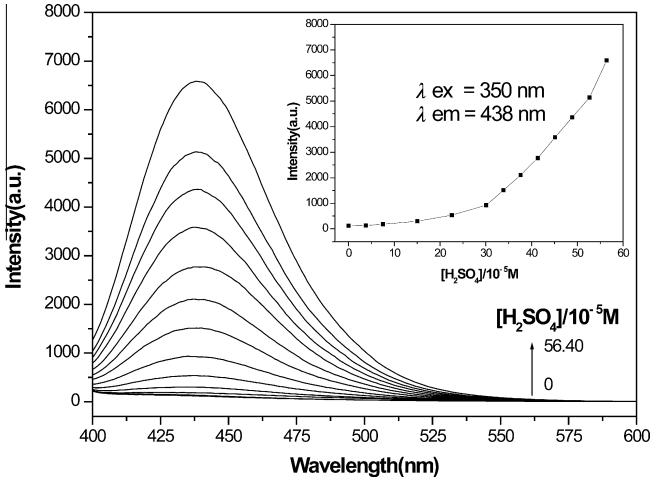

Fig. 9. Fluorescence spectra changes of **1c** in ethanol solution (2.16×10^{-6} M) upon addition of increasing concentrations of H_2SO_4 (0–56.40×10^{-5} M). *Inset*: fluorescence intensity at 438 nm as a function of H_2SO_4 concentration.

and then reduced (Fig. 7). Concurrently, a red-shift in the fluorescence maximum was observed (Fig. 7). From the fluorescence spectra of **1c** in ethanol with varying amounts of water, it could be seen that, when the water fraction was increased from 0% to 20%, the fluorescence intensity for **1c** shows only a slight increase. Upon the increasing of water content from 30% to 80%, **1c** exhibits a strong blue fluorescence emission peak with a significant fluorescence enhancement and a small red shift in its emission wavelength (from 441 to 451 nm). However, an obvious drop in the overall intensity and a slight red shift in its emission wavelength (from 451 to 454 nm) are observed when the water fraction was further increased from 80% to 90%. This means that more than 80% water content is not effective in enhancing the fluorescence properties. It was clear that compound **1c** had sensitive responses towards changes in the water composition in the aqueous solvent systems.

Additionally, this investigation has also been extended to the ethanol-heavy water (D_2O) systems. Similarly, in the case of ethanol–D_2O mixture (V_{D2O} = 80%) we also observe the enhanced blue fluorescence emission.

Besides, responses of **1c** to acid (e.g. HOAc and H_2SO_4) were also investigated. As can be seen in Figs. 8 and 9, upon the addition of acid, compound **1c** shows significant fluorescence enhancement, and exhibits a strong blue fluorescent emission peak at ca. 438–440 nm, which is blue-shifted with respect to the peak observed in the presence of water.

In sharp contrast, these fluorescence properties were not observed in the cases of **1a**, **1b**, and **1d**. Further testing, meanwhile, revealed that the fluorescence of **1c** was scarcely influenced by the addition of alkali (e.g. sodium hydroxide (NaOH) and tetrabutylammonium hydroxide (TBAH)).

As is mentioned above, addition of water to **1c** does not promote significant changes in the UV–vis spectrum in comparison with that observed in pure ethanol solution. However, the presence of H_2SO_4 had obvious effect on the absorption spectra of **1c**. Moreover, the absorption behavior of **1c** in the presence of H_2SO_4 also depends on the amount of H_2SO_4 added. Fig. 10 shows the effect of varying amounts of H_2SO_4 on the absorption spectra. From Fig. 10, one observes that the addition of a small amount of H_2SO_4 (9.4×10^{-5} M) to the system does not alter the shape and wavelength maximum of the absorption spectra for **1c** but can reduce the absorbance obviously. Further, with the increase in the amount of H_2SO_4, the observed two absorption bands at around

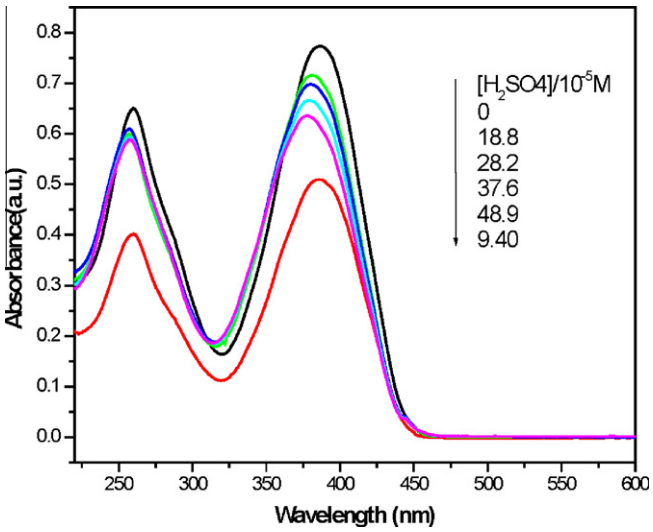

Fig. 10. Absorption spectra changes of **1c** in ethanol solution (2.16×10^{-5} M) upon addition of H_2SO_4.

260 and 387 nm were blue-shifted by 3 and 9 nm, respectively, with decreasing of the absorbance.

Such efficient emission enhancement for **1c** might be attributed, at least in part, to a change in the microscopic polarity around the fluorophore with increasing concentrations of water, HOAc or H_2SO_4 in ethanol [33,34]. Another possible reason for the increased fluorescence intensity in the ethanol/water mixtures is the formation of amorphous aggregates, which shows an aggregation-induced emission enhancement effect. Meanwhile, it is likely that the intramolecular photoinduced electron transfer (PET) process or the isomerization of C=N may be suppressed [22], leading then to enhancement of fluorescence emission. Of course, the bithienyl unit is thought to play a key role in affecting fluorescence intensity, though **1c** is almost non-fluorescent in ethanol. Nevertheless, it should be pointed out that more experiments must be carried out to estimate such hypothesis.

Conclusions

In summary, the synthesis and characterization for four new antipyrine derivatives are presented in this paper. X-ray structural analysis show **1b** to be monoclinic, space group $P2_1/c$. The bithienyl-antipyrine derivative **1c** exhibits interesting fluorescence responses to water, HOAc or H_2SO_4, but not to alkali. Upon the addition of water, HOAc or H_2SO_4, a remarkable fluorescence enhancement of bithienyl-antipyrine derivative **1c** was observed. The results may provide a useful framework for the development of effective fluorescence sensors.

Acknowledgement

This work is supported by the Nature Science Foundation of Shandong Province of China (No. ZR2010BM032).

References

[1] S. Bondock, R. Rabie, H.A. Etman, A.A. Fadda, Eur. J. Med. Chem. 43 (2008) 2122–2129.
[2] H.M. Aly, N.M. Saleh, H.A. Elhady, Eur. J. Med. Chem. 46 (2011) 4566–4572.
[3] M. Hartleb, Biopharm. Drug Dispos. 12 (1991) 559–570.
[4] S. Botros, R. Abdel-Kader, M. El-Ghannam, A. El-Ray, S. Saleh, M. Mahmoud, Int. J. Trop. Med. 2 (2007) 101–106.
[5] G. Ceriotti, Clin. Chem. 17 (1971) 400–402.
[6] E. Morita, E. Nakamura, Anal. Sci. 27 (2011) 489–492.
[7] Y. Fiamegos, C. Stalikas, G. Pilidis, Anal. Chim. Acta 467 (2002) 105–114.
[8] X.-P. Yang, B.-S. Kang, W.-K. Wong, C.-Y. Su, H.-Q. Liu, Inorg. Chem. 42 (2003) 169–179.
[9] P.M. Selvakumar, E. Suresh, P.S. Subramanian, Polyhedron 26 (2007) 749–756.
[10] T. Rosu, E. Pahontu, C. Maxim, R. Georgescu, N. Stanica, A. Gulea, Polyhedron 30 (2011) 154–162.
[11] A.K. Sharma, S. Chandra, Spectrochim. Acta A 81 (2011) 424–430.
[12] G.E. Shestakova, A.E. Lesnov, N.V. Bryzgalova, Radiochemistry 49 (2007) 171–173.
[13] M.I. Degtev, E.M. Nechaeva, Russ. J. Inorg. Chem. 52 (2007) 1295–1298.
[14] F. Mahle, T.R. Guimarães, A.V. Meira, R. Corrêa, R.B. Cruz, A.B. Cruz, R.J. Nunes, V. Cechinel-Filho, F. Campos-Buzzi, Eur. J. Med. Chem. 45 (2011) 4761–4768.
[15] S.A.F. Rostom, I.M. El-Ashmawy, H.A.A.E. Razik, M.H. Badr, H.M.A. Ashour, Bioorg. Med. Chem. 17 (2009) 882–895.
[16] T. Rosu, M. Negoiu, S. Pasculescu, E. Pahontu, D. Poirier, A. Gulea, Eur. J. Med. Chem. 45 (2010) 774–781.
[17] X.Y. Zhang, J. Chem. Crystallogr. 41 (2011) 1044–1048.
[18] N. Uramaru, H. Shigematsu, A. Toda, R. Eyanagi, S. Kitamura, S. Ohta, J. Med. Chem. 53 (2010) 8727–8733.
[19] T. Rosu, E. Pahontu, M. Reka-Stefana, D.-C. Ilies, R. Georgescu, S. Shova, A. Gulea, Polyhedron 31 (2012) 352–360.
[20] S. Cunha, S.M. Oliveira, M.T. Rodrigues Jr., R.M. Bastos, J. Ferrari, C.M.A. de Oliveira, L. Kato, H.B. Napolitano, I. Vencato, C. Lariucci, J. Mol. Struct. 752 (2005) 32–39.
[21] J.-S. Wu, J.-H. Zhou, P.-F. Wang, X.-H. Zhang, S.-K. Wu, Org. Lett. 7 (2005) 2133–2136.
[22] J.-S. Wu, W.-M. Liu, X.-Q. Zhuang, F. Wang, P.-F. Wang, S.-L. Tao, X.-H. Zhang, S.-K. Wu, S.-T. Lee, Org. Lett. 9 (2007) 33–36.
[23] Y.-F. Sun, D.-D. Zhang, H.-C. Song, Chin. J. Struct. Chem. 26 (2007) 511–514.
[24] Y.-F. Sun, J.-K. Li, Z.-B. Zheng, Acta Cryst. E63 (2007) o2520–o2521.
[25] Y.-F. Sun, J.-K. Li, Z.-B. Zheng, R.-T. Wu, Acta Cryst. E63 (2007) o2522–o2523.
[26] Y.-F. Sun, S.-H. Xu, R.-T. Wu, Z.-Y. Wang, Z.-B. Zheng, J.-K. Li, Y.-P. Cui, Dyes Pigments 87 (2010) 109–118.
[27] A. Adamczyk-Wozniak, M.K. Cyranski, A. Dabrowska, B. Gierczyk, P. Klimentowska, G. Schroeder, A. Zubrowska, A. Sporzynski, J. Mol. Struct. 920 (2009) 430–435.
[28] S.J. Rettig, J. Trotter, Can. J. Chem. 55 (1977) 3071–3075.
[29] P. Rogowska, M.K. Cyranski, A. Sporzynski, A. Ciesielski, Tetrahedron Lett. 47 (2006) 1389–1393.
[30] D. Bykowski, R. McDonald, R.J. Hinkle, R.R. Tykwinski, J. Org. Chem. 67 (2002) 2798–2804.
[31] B. Pedras, L. Fernandes, E. Oliveira, L. Rodríguez, M.M.M. Raposo, J.L. Capelo, C. Lodeiro, Inorg. Chem. Commun. 12 (2009) 79–85.
[32] Y.-F. Sun, Y.-P. Cui, Dyes Pigments 78 (2008) 65–76.
[33] B. Ramachandram, G. Saroja, N.B. Sankaran, A. Samanta, J. Phys. Chem. B 104 (2000) 11824–11832.
[34] B. Ramachandram, N.B. Sankaran, R. Karmakar, S. Saha, A. Samanta, Tetrahedron 56 (2000) 7041–7044.